

Review

Review of VHEE Beam Energy Evolution for FLASH Radiation Therapy Under Ultra-High Dose Rate (UHDR) Dosimetry

Nikolaos Gazis ^{1,2}  and Evangelos Gazis ^{1,3,*}¹ Institute of Accelerating Systems and Applications, 10300 Athens, Greece; nick.gazis@ess.eu² European Spallation Source-European Research Infrastructure Consortium, 22100 Lund, Sweden³ Physics Department, National Technical University of Athens, Zografou Campus, 15780 Athens, Greece

* Correspondence: egazis@central.ntua.gr

Abstract

Very-high-energy electron (VHEE) beams, ranging from 50 to 300 or 400 MeV, are the subject of intense research investigation, with considerable interest concerning applications in radiation therapy due to their accurate energy deposition into large and deep-seated tissues, sharp beam edges, high sparing properties, and minimal radiation effects on normal tissues. The very-high-energy electron beam, which ranges from 50 to 400 MeV, and Ultra-High-Energy Electron beams up to 1–2 GeV, are considered extremely effective for human tumor therapy while avoiding the spatial requirements and cost of proton and heavy ion facilities. Many research laboratories have developed advanced testing infrastructures with VHEE beams in Europe, the USA, Japan, and other countries. These facilities aim to accelerate the transition to clinical application, following extensive simulations for beam transport that support preclinical trials and imminent clinical deployment. However, the clinical implementation of VHEE for FLASH radiation therapy requires advances in several areas, including the development of compact, stable, and efficient accelerators; the definition of sophisticated treatment plans; and the establishment of clinically validated protocols. In addition, the perspective of VHEE for accessing ultra-high dose rate (UHDR) dosimetry presents a promising procedure for the practical integration of FLASH radiotherapy for deep tumors, enhancing normal tissue sparing while maintaining the inherent dosimetry advantages. However, it has been proven that a strong effort is necessary to improve the main operational accelerator conditions, ensuring a stable beam over time and across space, as well as compact infrastructure to support the clinical implementation of VHEE for FLASH cancer treatment. VHEE-accessing ultra-high dose rate (UHDR) perspective dosimetry is integrated with FLASH radiotherapy and well-prepared cancer treatment tools that provide an advantage in modern oncology regimes. This study explores technological progress and the evolution of electron accelerator beam energy technology, as simulated by the ASTRA code, for developing VHEE and UHEE beams aimed at medical applications. FLUKA code simulations of electron beam provide dose distribution plots and the range for various energies inside the phantom of PMMA.

Keywords: VHEE; electron accelerator technology; FLASH radiation therapy; ultra-high dose rate; dosimetry; ASTRA and FLUKA/FLAIR codes



Academic Editor: Andrew Stevenson

Received: 12 July 2025

Revised: 2 September 2025

Accepted: 11 September 2025

Published: 9 October 2025

Citation: Gazis, N.; Gazis, E. Review of VHEE Beam Energy Evolution for FLASH Radiation Therapy Under Ultra-High Dose Rate (UHDR) Dosimetry. *Quantum Beam Sci.* **2025**, *9*, 29. <https://doi.org/10.3390/qubs9040029>

Copyright: © 2025 by the authors.

Licensee MDPI, Basel, Switzerland.

This article is an open access article distributed under the terms and

conditions of the Creative Commons

Attribution (CC BY) license

([https://creativecommons.org/](https://creativecommons.org/licenses/by/4.0/)

[licenses/by/4.0/](https://creativecommons.org/licenses/by/4.0/)).

1. Introduction

It has recently been reported [1,2] that there will be a continuous increase in cancer incidents, from about 18 million to almost 30 million people over the coming years toward

2040, necessitating an advanced treatment method. Most cancer patients are treated with radiation therapy [3], an effective tool for treating cancer. A charged particle beam irradiates the tumor with a sufficient dose to eliminate tumor growth and minimize the damage to neighboring normal tissues. Figure 1 shows the energy delivery from the charged particle beam inside the matter [4]. Many charged particle irradiation-based therapeutic protocols have been developed, implementing proton/carbon ion therapy [5,6], very-high-energy electron—VHEE [7], and FLASH radiation therapy (FLASH-RT) [8,9]. FLASH radiotherapy represents an innovative approach to radiotherapy, exploiting the radiobiological mechanism known as the FLASH effect [10], offering the possibility of delivering an extremely high dose rate (>40 Gy/s) while minimizing adverse effects on healthy tissues and organs. This FLASH condition damages the cancer cells while causing minimal damage to healthy tissue. FLASH-RT, as a major feature in cancer treatment, was initially observed in 1966. A renewed interest in the method and application for treatment appeared in a novel work in 2014 [11].

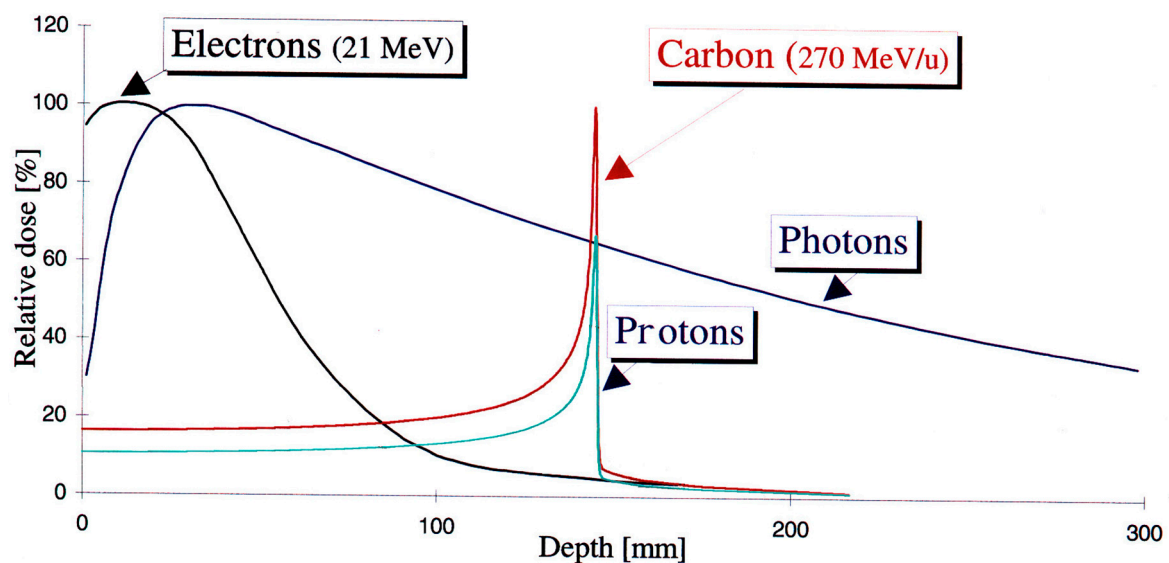


Figure 1. The charged particle beams' energy distribution versus the material depth of electrons, protons, and carbon ions compared to photon beam irradiation [4].

The development of a VHEE beam energy regime for FLASH radiation therapy with ultra-high dose rate (UHDR) dosimetry has been reported by accelerating facilities in the large High-Energy Physics (HEP) laboratories in Europe, the USA, Japan, etc., where therapeutic schemes are examined according to the electron energy domain [12]. New scientific collaboration consortia have been launched during the last ten years, including the CLEAR collaboration: (CERN Linear Electron Accelerator for Research) [13] in Switzerland, the PRAE: Platform for Research and Applications with Electrons project [14–16] in France, the ASTEC CLARA: (Compact Linear Accelerator for Research and Applications) [17] in the UK, the SPARC at LNF-INFN [18] in Italy, and others elsewhere. The purpose of these collaborations is to establish novel linear accelerator structures for electron beams, increasing their energies to some hundred MeV, creating testing facilities with ultra-brilliant electron beams that lead to FEL-intense radiation for scientific and industrial use, or to VHEE for medical applications. Applications focusing on tumor treatment involve simulation studies of various parameters to determine the dose dependency on beam spot dimension, the beam central axis percentage-depth-dose (PDD), the source-to-surface distance (SSD), and the relative technical challenges involved, as extensively reported [2]. Additional operation condition parameters of the accelerator enhance the radiobiological

experimental capabilities, defining a state-of-the-art technological design for future planned VHEE FLASH experiments [19].

There has been renewed interest in VHEE facilities, driven by the increase in electron beam energy in the GeV era, due to the innovative technology of compact, high-gradient, high-brightness RF-based and/or plasma wakefield accelerators [20].

Wakefield accelerator technology provides a compact, size- and cost-efficient improvement for the high-energy electron beam production [21], which can provide similar dose distributions to photon beams while using more intense and more precise electron beam bunches [22,23].

Laser wakefield accelerators have a significant advantage in delivering FLASH (ultra-high dose rate) irradiation. The FLASH effect can be achieved under fixed beam parameter conditions [24], providing flexible modulation of beam parameters proper for FLASH-VHEE treatment, leading to an exciting project for cancer therapy. In Table 1, the beam characteristic conditions of the conventional electron beam irradiation vs. the FLASH-RT effect are summarized [2,11,12,25,26].

Table 1. Beam characteristic conditions of conventional electron beam irradiation vs. the FLASH-RT effect [11,12].

Beam Characteristics	Conventional RT	FLASH RT
Dose Per Pulse	~0.4 mGy	>1 Gy
Dose Rate	~10 ² Gy/s	~10 ⁵ Gy/s
Mean Dose Rate	~0.1 Gy/s	~100 Gy/s
Total Treatment Time	~seconds	<500 ms

The FLASH-RT effect conditions for a dose >1 Gy are generally considered, which is many orders of magnitude greater than usual conventional radiation therapy via an electron pulse dose (<1 mGy/pulse) [2,11,12,25,26]. The FLASH-RT conditions defined for beam irradiation have the following necessary operational parameters [13,14,27,28]:

- Irradiation time: $t_i < 100$ ms;
- Average dose rate: $\bar{D} > 100$ Gy/s;
- In-peak dose rate: $\dot{D}_p > 10^6$ Gy/s;
- Pulse repetition frequency: PRF > 100 Hz;
- Dose per pulse: >1 Gy.

2. VHEE Beam Energy Evolution to Treatment

The implementation of very short pulses of ultra-high dose rate FLASH radiation therapy under new protocols includes important radiobiological advantages [11], which can be facilitated by recent innovative technological developments available with the new generations of developed accelerators. There has been tremendous accelerator technology progress with recent advantages providing compact, low-cost, and best performance facilities with high-gradient cavities, realizing possible enrichment for medical applications. Very-high-energy electron (VHEE) radiation therapy, in the energy range of 50 to 300 MeV, started around the year 2000, being particularly accurate and minimally affecting healthy tissues, making it applicable in many deep anatomical tumor areas [29], has also been confirmed to be less expensive than hadron therapy facilities (protons or carbon ions). It should be noted that hadron therapy and electron FLASH radiotherapy are advanced techniques offering precise tumor targeting and reduced healthy tissue damage, acting via different mechanisms on tissues. Hadron therapy (protons and carbon ions) provides superior physical precision through Bragg peak localization and can deliver a very-high-energy dose directly to the tumor, with less exit dose, while FLASH-RT spares healthy tissues

from radiation damage and maintains tumor control efficacy through ultra-high dose rates. Electron FLASH, although requiring new technology, provides similar biological effects and tissue sparing, similar to hadrons, and focuses on reducing toxicity. In Table 2, a step-by-step comparison is shown of hadron therapy vs. electron FLASH-RT dosimetric and biological factors across modalities and other parameters [30,31].

Table 2. Step-by-step comparison of hadron therapy vs. electron FLASH-RT in various factors.

Factors	Hadron Therapy	e-FLASH RT
Mechanism	hits the tumor volume by causing heavy particles to deposit; most energy is in a specific tumor location	reduces toxicity through high dose rates, sparing the health tissues
Biological	provides high linear energy transfer (LET), effective against radio-resistant tumors	maintains effectiveness against tumors due to the ultra-fast delivery time of beam pulse
Precision	offers superior physical targeting and dose distribution for deep-seated tumors	offers a biological advantage in sparing healthy tissues
Technology	uses established accelerator technology: cyclotron or synchrotron	a new generation of linear electron compact accelerator is needed with very high intensity and ultra-fast beam pulse
Applications	ideal for deeply located and inoperable tumors	treats skin cancer and soft tissue sarcomas
Size–Cost	a hadron synchrotron has a sizeable diameter of about one hundred meters and costs hundreds of millions of EUR	an electron linac is tens of meters in length and costs tens of millions of EUR

VHEE performs tumor treatment via electron beam scanning, guided via electromagnets, with high doses per fraction, thereby improving its effectiveness in terms of damage. The most characteristic feature to be taken advantage of is the FLASH effect conditions, which involve very-high-dose beam irradiation of tissues in an extremely short time, thereby preventing the increase in early and late complications of malignant tumors that affect normal tissues, while the tumor remains under control.

The evolution of the current knowledge on ultra-high dose rate VHEE radiation therapy is presented in the literature, considering the probable future implementation of VHEE therapy for clinical treatment. The advances of the two novel radiation therapy treatment combinations, UHDR and VHEE, have been made, meaning the very-high-energy electron (VHEE) beam under FLASH condition radiation therapies, for a single treatment beam shot, results in a substantial change in the field of radiotherapy, resulting in fewer therapeutic problems for patients [32].

Many years have passed since the use of electron beams by medical linacs for radiation therapy, dating back to the early 1950s. Treatment examples include the breast, chest, skin, eyes, salivary glands, or parts of other organs, and are considered a complementary method to the usual photon radiation therapy [33]. Many new techniques were developed using electron beam collimation, which involved adapting multi-leaf collimators (MLC) to remove the field shaping cut-outs, typically mounted on electron applicators near the patient [34]. A very common application of electron beam is the intraoperative technique (IOERT), consisting of the application of a dose during or after operation on the tumor tissue with electron beam energies between 4 and 12 MeV [35].

A real technological and radiotherapeutic revolution is in progress, as many of the existing low-energy electron linacs have been modified or new ones have been designed to be used after the discovery of the new dynamic treatment methodology—FLASH radiation therapy [11,36].

The VHEE under ultra-fast time pulse radiation treatment implements extremely high dose rates, orders of magnitude greater than those usually used. It has recently been published that the efficiency of FLASH radiation therapy with electrons for inhibition, sparing healthy tissue, has been demonstrated [37,38]. The major advantage of the FLASH treatment is sparing normal tissues from the observed late complications after radiation therapy at a conventional dose rate, while maintaining efficiency against volumes unchanged. Normal tissue sparing by FLASH has been verified for most organs in small animal tests. The underlying biological effect mechanisms must be elaborated; the FLASH treatment effect has also been confirmed in a human tumor, supporting further studies and clinical trials following the promising results obtained [9].

There is a general effort for the beam parameters related to the beam pulse length, the mean dose rate, the total dose, and the total irradiation time to be optimized to improve clinical results without departing from the adopted standard specifications for the FLASH effect, e.g., >1 Gy and 10^6 Gy/s, respectively; a pulse repetition rate of a few tens of Hz; and a total irradiation time less than 100 ms. A significant research effort emerged, aiming to fulfill the conditions for the FLASH effect using various novel technology options. This included the development and design of the fourth-generation FEL accelerator, as in the case of the CompactLight [39,40] and EuPRAXIA PP collaborations [41,42]; laser-driven accelerators, which are considered as the subsequent cost-effective accelerator generation for radiotherapy [43]; and very-high-energy electrons (VHEEs) that have an electron beam energy of more than 100 MeV [44]. Most recent works refer to electrons for the FLASH effect, with a beam energy sufficient to deliver radiation to the proper tissues.

However, due to the innovative achievements in high-gradient accelerator technology in recent decades, VHEE radiation therapy involves the use of electron beams in the energy range of 100–350 MeV and above. A complications research study focused on beam delivery and treatment planning [25] with Monte Carlo simulations using the Tool for Particle Simulation—TOPAS/GEANT4 (TOPAS tool for particle simulation: (<https://www.topasmc.org/home>, accessed on 10 September 2025); the code indicates increased tissue penetration results versus low-energy electrons. The on-axis percentage depth dose (PDD) simulation curves TOPAS/GEANT4 for radiotherapy modalities are shown in Figure 2a, with 15 and 200 MeV electrons, 6 MV photons, and 200 MeV protons. The simulation was performed assuming a Gaussian beam of standard deviation $\sigma = 2$ mm, incident on a $30 \times 30 \times 30$ cm³ water phantom with $301 \times 301 \times 301$ bins of 10^6 , 10^7 , and 10^8 histories for protons, electrons, and photons, respectively. As shown in Figure 2b, the reduced lateral spread of the Gaussian electron beam with increased energy compared to lower-energy electrons is further demonstrated across several electron beam energies. The lighter particles also have the potential for rapid treatment delivery by scanning the beam over the tumor area, activating electromagnetic systems [19].

Several studies at the CLEAR facility at CERN indicate that VHEE beams have a reduced sensitivity to tumor inhomogeneities compared with other charged particles, such as protons, resulting in lower doses in regions heterogeneous to healthy tissue, such as the lung or prostate, in a clinical setting [45]. Currently, deep-seated tumors are usually treated due to the development of high-gradient accelerator technology achievements, where the increasing interest is in using very-high-energy beams able to penetrate to 20–50 cm depths inside the patient's body [46]. The dosimetry properties of particle beams at various density region interfaces are essential for planning and delivering optimal radiation therapy to patients. The possible discrepancies in high- and low-density regions in the irradiation volume, i.e., the lung, can significantly alter the delivered dose distribution. These dose range uncertainties caused by such volume inhomogeneities may affect parts of the tumor, sometimes resulting in significant under- or over-dosing.

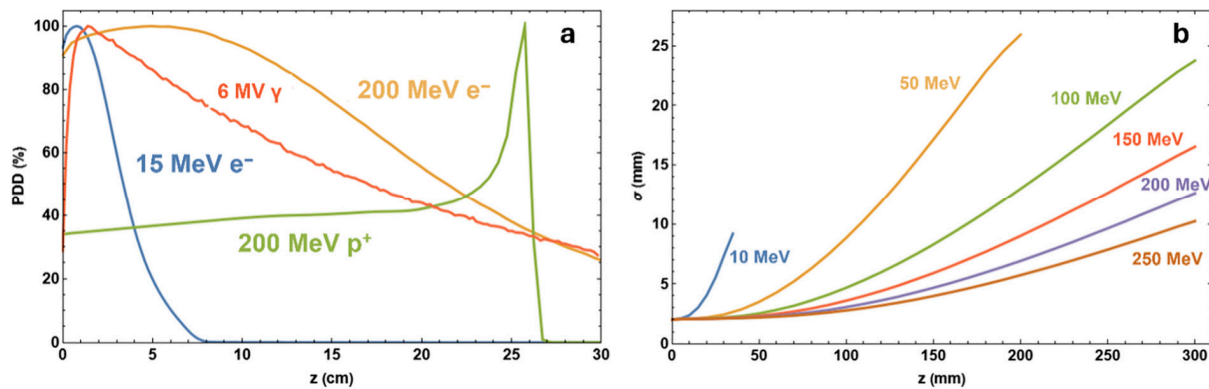


Figure 2. (a) On-axis percentage depth dose (PDD) simulation curves TOPAS/GEANT4 for radiotherapy modalities. (b) Lateral spread of Gaussian electron beam simulations; data include 10^7 particles [19].

Recently, there has been a real increase in interest in VHEE methodology due to the novel technological benefits, which overcome many problems initially faced in the VHEE accelerators. The major problem was the necessary large size of the linear accelerator (LINAC) needed to obtain such high-energy electron beams of 1 GeV or more. Simulation studies have shown that these beam energies produce dose distributions comparable to those of photon beams. The delivery of electron beams provides advantages over photon radiation due to their more precise manipulation with fewer facility components and much shorter pulse time duration, with more intense electron bunches. It is underlined that the FLASH effect can only be exploited under certain beam parameter conditions, with the flexibility of the modulation of the electron beam parameters provided by these accelerators for FLASH-VHEE treatments presenting an exciting prospect [24,36].

The double differential scattering cross-sections (DDSC) are inversely proportional to the beam electron energy squared. Therefore, various scattering effects within the patient's body are relatively reduced by increasing the beam energy. So, the VHEE beam spot is much sharper for lower depths and increases for deep-seated targets. Additionally, simulation results exclusively for the case of the Ultra-High Energy Electron (UHEE) beams up to 1.2 GeV [47], determine the relative biological effectiveness (RBE) by assessing the cell survival of healthy and tumor tissue damage. It has been reported that the VHEE beam dose is not affected by tumor volume characteristics such as the surface obliquity or depth heterogeneity. The VHEE beam dose indeed maintains a sustained dose uniformity at organ-tissue interfaces for various tissue densities, including lung, muscle, bone, fat, and air cavities [48]. Subsequently, this has been experimentally confirmed at CERN [45]. It should be mentioned that the VHEE-FLASH lacks a clinical translation roadmap as a viable clinical treatment for deep-seated tumors, requiring stable operational parameters for VHEE systems designed for ultra-high dose rate delivery. Although low-energy electron beam accelerators have been modified for FLASH radiation therapy for skin, a general effort for FLASH radiotherapy development is aimed at a dynamic solution based on RF-cavity modification of conventional accelerators and/or on innovative laser/beam-driven plasma accelerators. In addition, VHEE clinical accelerator specifications for application to clinical protocols have started to take place in these directions [49].

3. Current VHEE Facilities

The major European VHEE facilities currently available, or under development/upgrading, are focusing, after their operation, on FLASH capabilities for radiobiological applications or clinical treatment, and are presented below:

- (i) CLEAR—CERN Linear Electron Accelerator for Research, CERN, Switzerland, operational since 2017. Electron beam energy range of 60–220 MeV [50,51].
- (ii) ARES—Accelerator Research Experiment at SINBAD, DESY, Germany, operational since 2022. Electron beam energy range of 50–155 MeV [52,53].
- (iii) CLARA—Compact Linear Accelerator for Research Applications, STFC, Daresbury Laboratory, UK, Phase 2 of the CLARA beamline, operational in the second half of 2025. Electron beam energy range of 50–250 MeV [54–57].
- (iv) SAFEST—SApienza FLASH Electron Source for radioTherapy, INFN, Italy, currently under development. Electron beam energy range of 80–100 MeV [58,59].

Table 3 summarizes the VHEE facilities' beam parameters, including the relative energy range (MeV), bunch charge (nC), pulse repetition frequency (Hz), and beam size range, providing flexibility in accelerator design for proper beam delivery.

Table 3. Major key parameters for European VHEE beam facilities [19].

Beam Parameter	CLARA	CLEAR	ARES	SAFEST
Energy Range (MeV)	50–250	60–220	59–155	80–100
Bunch Charge (nC)	0.005–0.25	0.01–1.5	0.00001–0.2	200
Relative Energy Spread	0.01% (low charge) 0.1% (high Charge)	<0.2%	0.039%	0.2%
Pulse Repetition Frequency (Hz)	1–100	0.8–10	1–50	100
Micro-bunches per Train	1	1–150	1	n/a
Beam Exit Window	250 μm Be	100 μm (Al)	50 μm (Ti)	n/a

4. FLASH Electron Beam Injector Simulation Studies

The FLASH effect requirements (see Table 1) define the necessary dose and irradiation time, enabling the accelerator system design constraints and proper technical challenges. Similar photocathode and laser system design parameters are also defined.

Simulation results are produced for the optimum electron accelerator setup parameters, as shown in Table 4, using a laser-irradiated photocathode obtained via the ASTRA code to obtain FLASH radiation therapy electron beam characteristic specifications [2].

Table 4. The ASTRA simulation results for laser and photocathode parameters to achieve the conditions for the FLASH-RT electron beam.

Parameters	Unit	Value
Photocathode material	-	Cs ₂ Te
RMS laser spot size (XY)	mm	0.90
Laser pulse duration	ps	10.00
Laser rise/fall time	ps	7.00
Laser wavelength	nm	262.0 (UVC)
Laser photon energy	eV	4.73
Initial kinetic energy	eV	1.61
Beam charge	nC	1.00
Electric field applied at cathode	MV/m	99.00
Beam energy distribution		Isotropic
Beam longitudinal distribution		Uniform Ellipsoid
Beam transverse distribution		Radial

The ASTRA code (Space Charge Tracking Algorithm) for the electron beam injector simulation parameters was used. ASTRA is an open-source software package developed at DESY (DESY Research Centre, https://desy.de/index_eng.html, accessed on 10 September 2025), which simulates beam generation and particle tracking via electromagnetic fields of

magnets, solenoids, cavities, etc. [60]. ASTRA particularly and successfully simulates the space charge-dominated beam effects applicable to our study, resulting in a properly generated beam profile. The relevant accelerator lattice optimizes emittance. In many works, a well-defined alignment between ASTRA simulations and experimental measurements is underlined [61–63].

One of the most important accelerator components is the photocathode material, which plays a definitive role as a parameter in an RF photoinjector. The well-selected photocathode material defines the quantum efficiency (QE) of the electron source and consequently the intrinsic emittance. Semiconductor materials, such as Caesium Telluride (Cs_2Te), are among the most efficient candidates for the photocathode, providing a quantum efficiency (QE) that is much larger in magnitude than metal photocathodes, i.e., copper (Cu) or magnesium (Mg). However, many operators prefer metal photocathodes due to their huge operational time relative to semiconductors [58]. In Figure 3, the electron accelerator block diagram is presented, with a total length of 9.5 m, providing an electron beam energy of 128.3 MeV. The accelerator features a Cs_2Te photocathode and an RF gun with a 100 MV/m gradient, which inserts the beam into two S-band accelerating structures that each house a strong, homogeneous magnetic solenoid. A short-length RF e-gun solenoid just after the photocathode and an injector solenoid with four parts in sequence were selected to optimize the beam emittance. The ASTRA simulation results for the electron beam energies 128.3, 446.1, and 1200 MeV are presented in Figures 4–9, with the proper important parameters for the optimum injector operation. It is underlined that the simulated electron beam energies 128.3 and 446.1 MeV were not extracted, as they were exactly foreseen to be 120 and 450 MeV due to the S-band cavity length, providing final shifted beam energies.

In this study, the following are presented: (i) The produced longitudinal electric field E_z (MV/m) in Figure 4, which produces an impressive homogeneity for a proportional electron beam acceleration. (ii) The injector solenoid with four sub-parts in sequence per S-band structure provides a homogenous solenoid field B_z (T), shown as a black line, and the magnetic field gradient dB_r/dr (T/m), shown as a red line vs. the beam axis for the first 5 m injector length. The magnetic field was adequately focused on the electron beam after the photocathode along the injector. Additionally, (iii) the transverse emittance is presented, where the electron beam is stabilized after the first 75 cm from its production, continuing to the beamline. (iv) The average beam energy is also shown from the photocathode to the injector for the first 9.5 m of acceleration, with its characteristic proportionality after a 1 m distance from the source, arriving at a final beam energy of 128.3 MeV. The transverse emittance seems to be constant with a low value after some initial oscillations in the first 2 m length of the injector, which is foreseen due to the e-gun beam output.

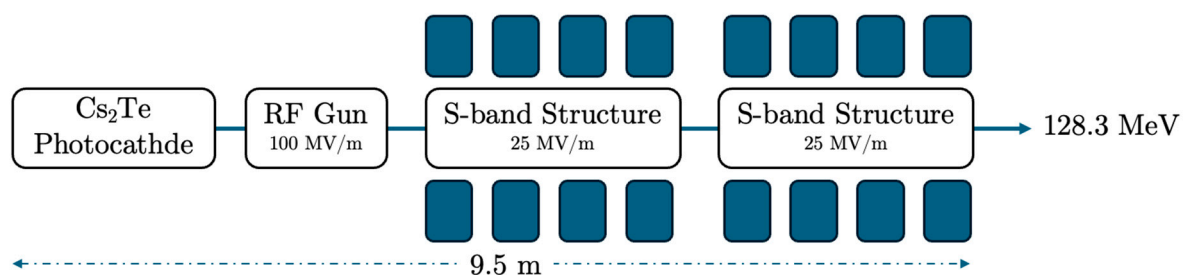


Figure 3. The electron beam accelerator setup has an energy of 128.3 MeV, with a photocathode, RF-gun, and 2 S-band cavities housed in a solenoid. The total injector has a length of 9.5 m.

The final simulation results obtained at the beam energy of 128.3 MeV, with the specific characteristics of the e-gun and the injector elements presented in Figure 4, support the

FLASH-RT electron beam specifications presented in Table 3, which were necessary for the electron dosimetry simulations. Figure 5 presents major output beam distribution plots produced via the ASTRA code, with the Cs₂Te photocathode, in terms of transverse phase-space vs. z -axis (mm) and z -axis (mm), plus the transverse distribution vs. the x and y axis, respectively, for the beam energy of 128.3 MeV.

The simulation results in Figure 5 show a broader distribution of the transverse phase-space vs. the axes x and y due to the much higher beam energy of 128.3 MeV, instead of the similar results near the e-gun [61] with better beam focusing. The transverse distribution vs. the axes x and y has a symmetrical beam distribution.

Similar simulation results are presented in Figures 6–8 with a final beam energy of 446.1 MeV.

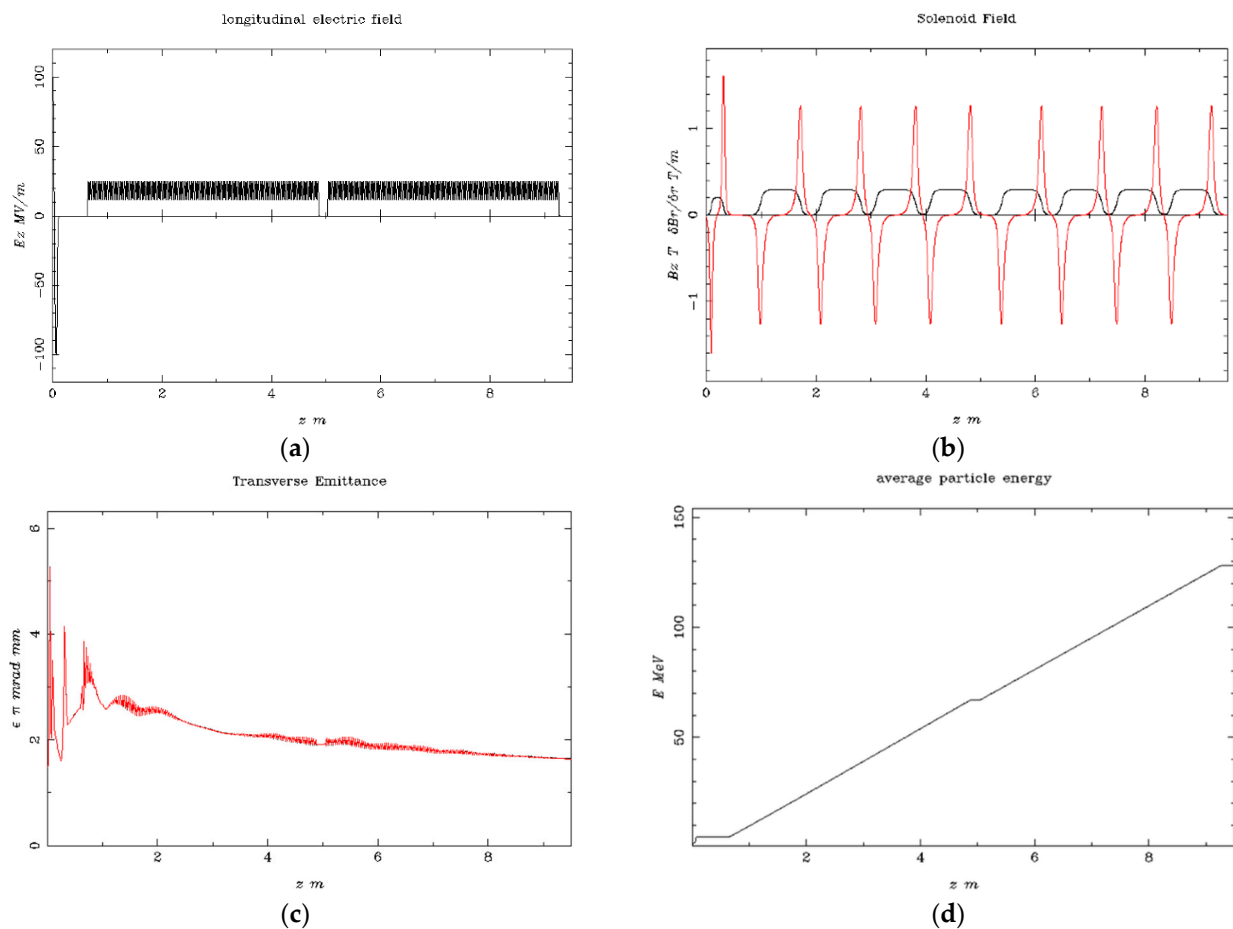


Figure 4. Simulation results at the beam energy of 128.3 MeV (a) the longitudinal electric field E_z (MV/m) vs. the beam axis z (m); (b) the solenoid field B_z (T) is shown as the black line, and the magnetic field gradient dBr/dr (T/m) is shown as the red line vs. the beam axis z (m) at the injector; (c) the electron beam transverse emittance vs. the beam axis z (m); (d) the average electron beam energy to the final stage.

The resulting beam parameters shown in Figure 7 for a beam energy of 446.1 MeV are quite similar to those in Figure 4. There is also (i) homogeneity for proportional electron beam acceleration. (ii) The two injector solenoids, each having four parts housing an S-band structure, produce a homogenous solenoid field B_z (T), shown as a black line, and the magnetic field gradient dBr/dr (T/m), shown as a red line vs. the beam axis for the first 10 m injector length. The magnetic field was adequately focused on the electron beam after the photocathode along the injector. Additionally, (iii) the transverse emittance is shown, where the electron beam is stabilized after the first 2 m from its production and

continues to the beamline; (iv) the average beam energy is also shown for the injector length of 27.5 m from the photocathode, with its characteristic proportionality after 1 m from the photocathode, arriving at a final beam energy of 446.1 MeV. The transverse emittance seems to be constant, with a low value after some initial oscillations in the first 2 m length of the injector, which is foreseen due to the e-gun beam output.

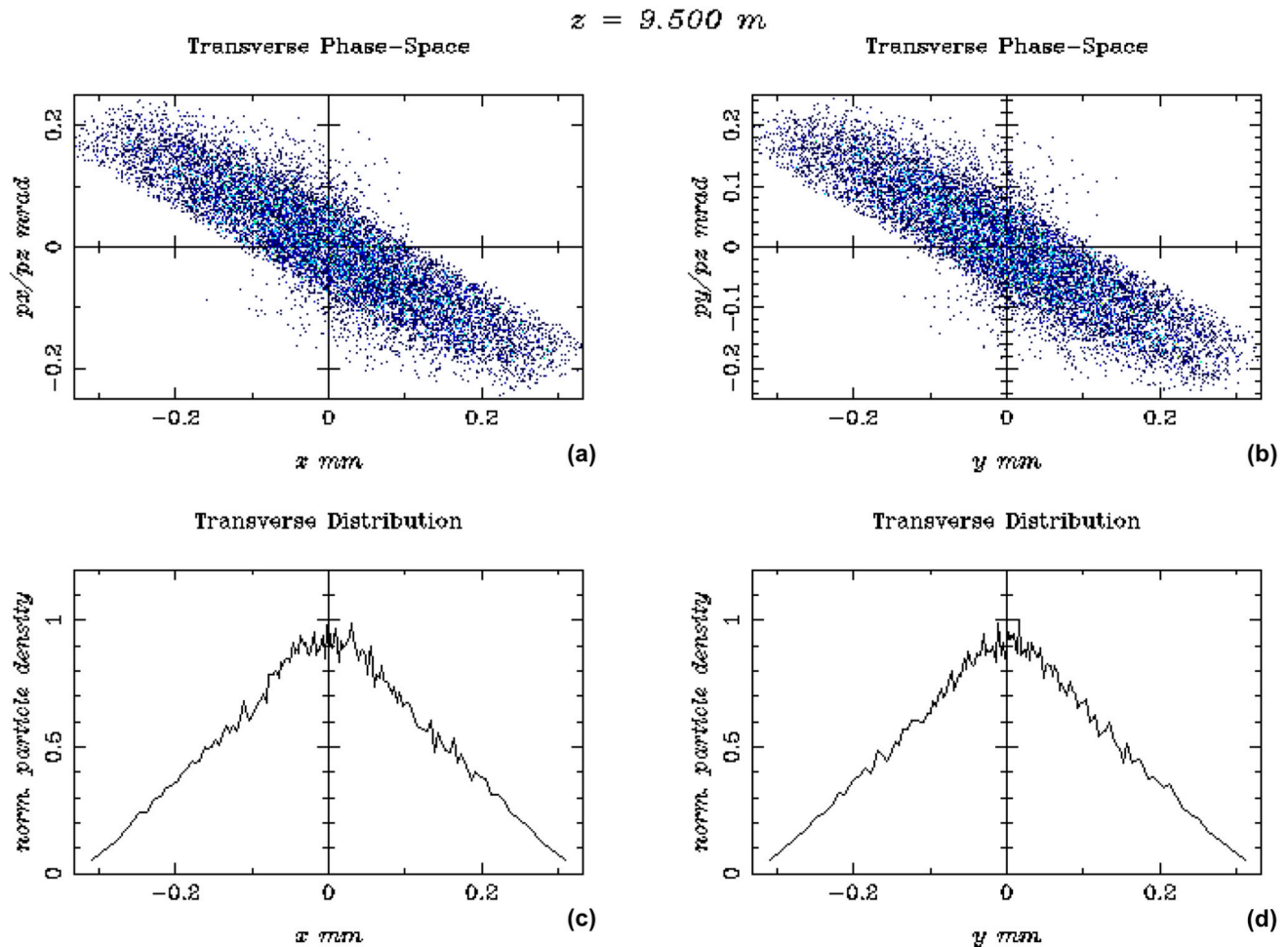


Figure 5. The output beam distributions, at the beam energy of 128.3 MeV, are shown in terms of (a) Transverse Phase-Space vs. z -axis (mm) and (b) y -axis (mm), plus (c) the transverse distribution vs. x -axis (mm) and (d) y -axis (mm).

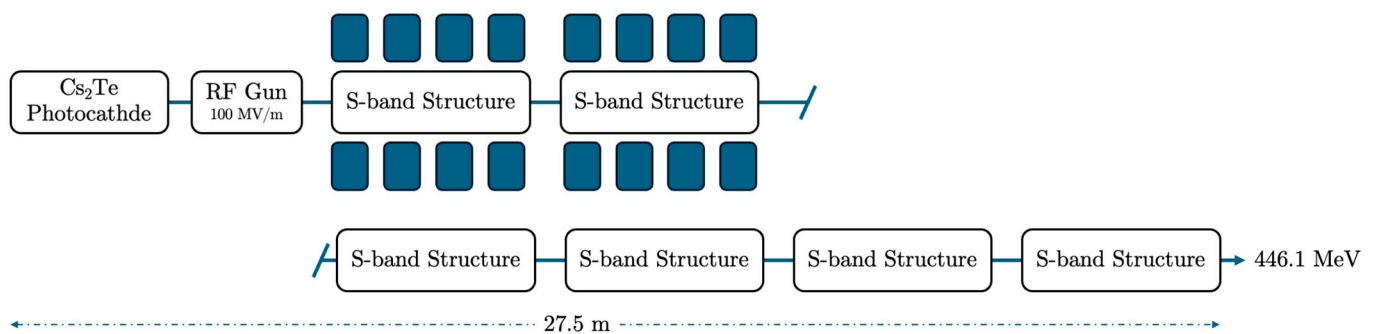


Figure 6. The electron beam accelerator setup of energy 446.1 MeV, with photocathode, RF-gun, and 2 S-band cavities housed in a solenoid, each one accompanied by four additional S-band structures. The injector has a total length of 27.5 m.

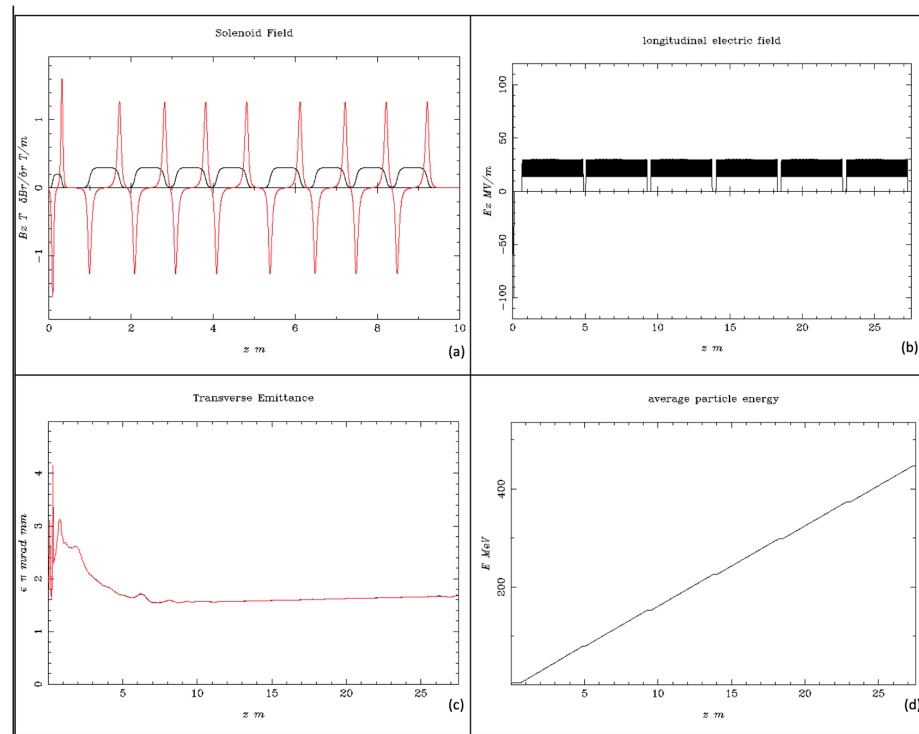


Figure 7. Simulation results for the beam energy of 446.1 MeV. (a) The solenoid field B_z (T), shown as the black line, and the magnetic field gradient dBr/dr (T/m), shown as the red line vs. the beam axis z (m) at the injector; (b) the longitudinal electric field E_z (MV/m) vs. the beam axis z (m); (c) the electron beam transverse emittance vs. the bam axis z (m); (d) the average electron beam energy to the final stage.

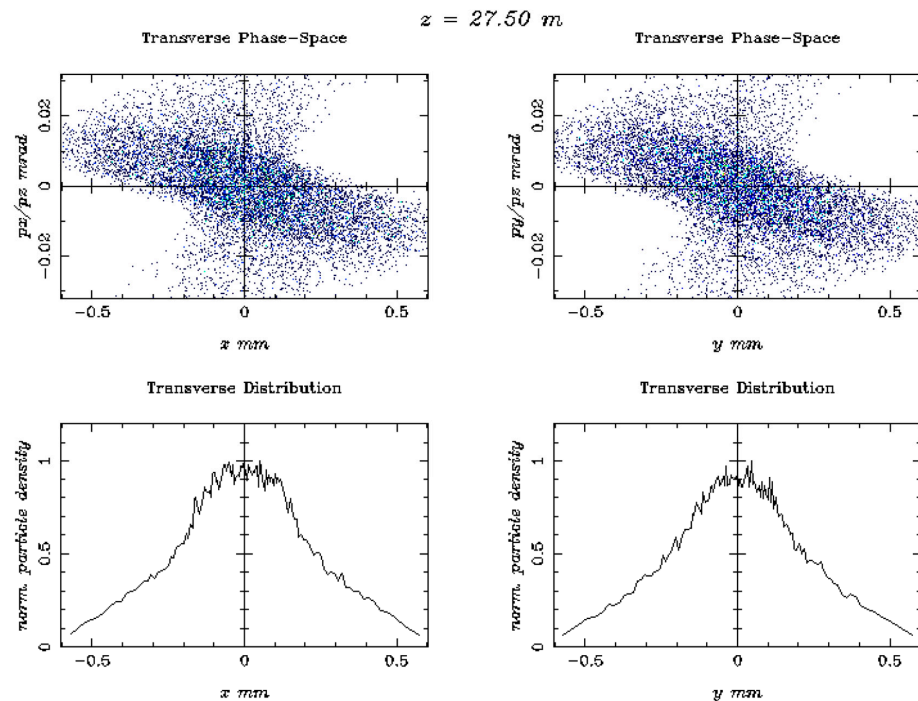


Figure 8. The output beam distributions, for the beam energy of 446.1 MeV, are shown in terms of Transverse Phase-Space vs. z -axis (mm) and z -axis (mm), plus the transverse distribution vs. x -axis (mm) and y -axis (mm).

Figure 8 presents the major output beam distribution plots produced via the ASTRA code, with a Cs_2Te photocathode, in terms of transverse phase space vs. the z -axis (mm)

and the z -axis (mm) plus the transverse distribution vs. the x and y axes, respectively, for a beam energy of 446.1 MeV. These beam distribution output results are much broader on the transverse phase space vs. x -axis (mm) and y -axis (mm) due to the much higher energy of 446.1 MeV.

Similar simulation results can be obtained for a beam energy of 1.2 GeV, which confirms the possibility of achieving a VHEE condition for FLASH RT with a relatively lower cost than other electron accelerators using X-band cavities and a more expensive RF supply.

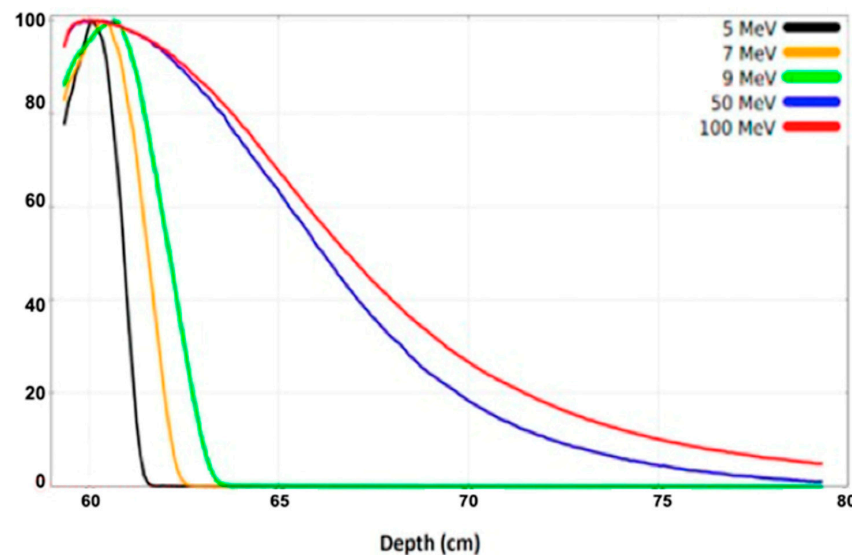


Figure 9. The percentage depth dose (PDD) plots for the electron beam energies of 5, 7, 9, 50, and 100 MeV, normalized to their maximum dose value [2].

5. Beam Dose Distribution Simulation Studies

Simulation studies for the beam dose rate and other parameters have usually been performed via variation of the experimental setup geometry, beam charge current, repetition rate, etc.

An accurate, user-friendly code is the TOPAS (Tool for Particle Simulation), based on the GEANT4 particle tracking code, properly implemented for large LHC experiments. Some characteristic simulation results of the 2D beam dose distribution, with the FLUKA code [64] for 5, 7, 9 MeV and higher electron energies of 50, 100 MeV, and 1.2 GeV, are presented in Figure 9 [2]. The FLUKA is a well-established code [65] that provides simulations in the context of electron FLASH radiation therapy, particularly for dose distributions and other dosimetric properties in water phantoms and other materials, confirmed with experimental measurements [27,66,67].

The basic longitudinal dosimetric parameters of the electron beam are summarized: (a) d_{\max} is the depth where we have the maximum dose deposition; (b) the therapeutic range (TR) is at 90% of D_{\max} , which is optimized for an ideal parallel beam. The therapeutic procedure ensures that the tumor is positioned steeply within the dose peak region of the beam, effectively sparing the healthy tissues surrounding the tumor. In addition, the characterized transverse parameters of the electron beam include the lateral penumbra (LP), representing the distance between the 20% to 90% intensity levels, and the beam width (BW), the width at 90% of the maximum dose value at a certain depth. Intensity levels are typically normalized to the maximum dose value [7].

The shapes of the depth–dose curves for various electron beam energies, in Figure 9, are similar, defined by useful range parameters. At low beam energies penetrating low- Z materials, the X-ray background is negligible. In the very-high-beam energy at 50 and

100 MeV, the PDD curve differs significantly from the low-energy one, penetrating to a depth of 80 cm inside the phantom [2]. The simulated results obtained with the applicator and phantom, both made from PMMA material (PMMA: Polymethyl Methacrylate is primarily used as a tissue-equivalent phantom material due to its similar radiation attenuation properties to human tissue and its high optical clarity) [67], are presented in Figure 10 [2]. These 2D dose distribution plots, with a range of electron energies of 50, 100 MeV, and 1.2 GeV, show the beam distribution inside the PMMA, simulating human tissue, with the VHEE beam increasing. It should be taken into consideration that at the 2D plot for the 1.2 GeV beam energy, the phantom dimension has been increased at the beam (z axis) to 140 cm, as the phantom size has a length of 100 cm for the two other lower energies. The peak of the beam energy absorption occurs within the phantom volume at approximately 10 cm, with a penumbra of 5 cm radius for 50 MeV. It then occurs at 20 cm, with a penumbra of 10 cm radius for 100 MeV, and at 110 cm, with a penumbra of 30 cm radius for 1.2 GeV. These results may be especially useful for deep-seated and flattened tumor radiation therapy, considering the beam energy distribution broadening that occurs within the tumor.

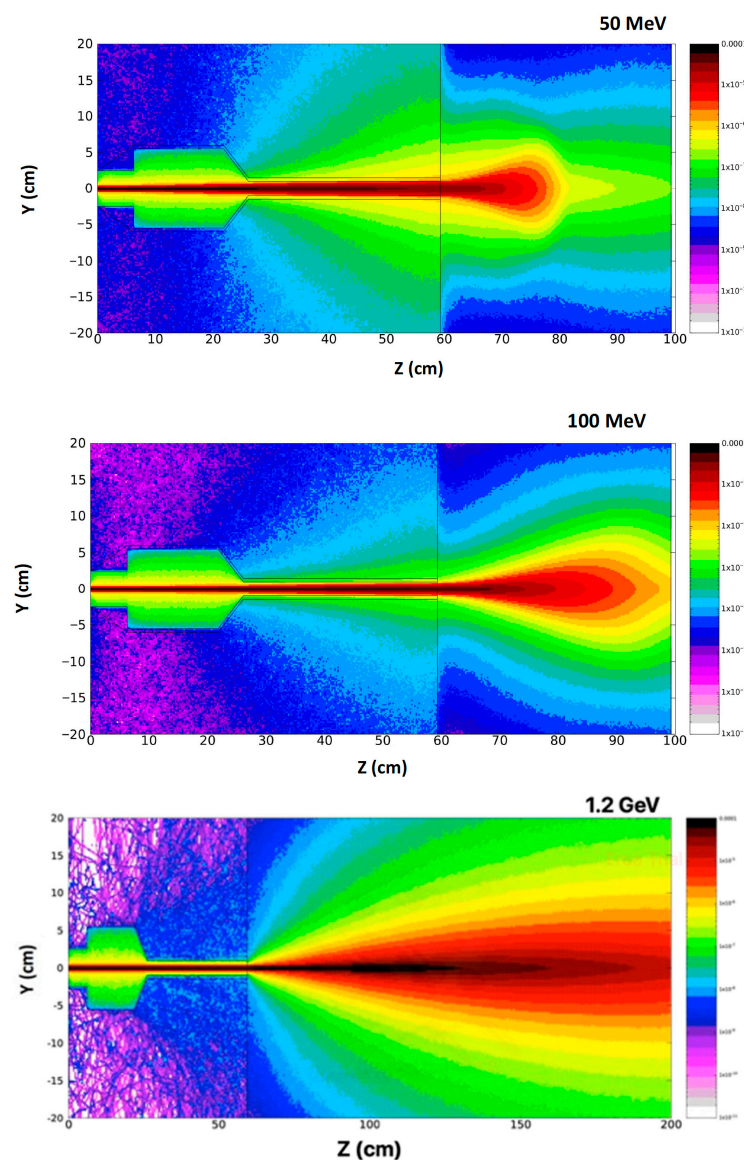


Figure 10. Simulation 2D dose distribution plots uncovered with FLUKA code using a range of electron energies, including 50, 100 MeV, and 1.2 GeV. It is underlined that the phantom dimension has been increased along the z-axis to 140 cm for the case of 1.2 GeV beam energy [2].

6. Radiation Safety

The general concept of ionizing radiation hazards is associated with the operation of an accelerator facility, which produces ionizing radiation, regardless of the type of accelerated particles or energy. There is a huge range of applications and the important benefits of the accelerators covering many different fields, especially in medical applications of diagnosis with short-lived radioisotopes and therapy with various beams, product sterilization, security access control, industrial radiography, communication broadcasting, and fundamental research, such as ultra-high energy colliding beam accelerators or applied research (synchrotron light sources). Extremely special care is taken during the VHEE-FLASH radiation therapy procedure to ensure the safety of the accelerator, medical personnel, and treated patients, as well as to minimize unwanted radiation exposure from scattered or secondary particles, including neutrons and photons. The main safety measures focus on time, distance, and shielding. Personnel should limit time in radiation areas, increase distance from the source, and use appropriate shielding, like lead or concrete. The measurement and control of radiation is monitored with dosimeters and other specialized devices, helping monitor exposure to protect against radiation hazards. Shielding is particularly crucial for secondary particles like neutrons and photons, which are produced when the primary beam interacts with matter [68].

7. Conclusions

The experimental range of electrons in matter depends on the beam energy and beam width due to the lateral scattering of electrons in matter. Similarly, the VHEE dose profile depends on the electron beam energy and beam width. The beam spread and the central-axis dose information from dose distributions perpendicular to the beam, and recorded in water at various depths, have been studied [2,8,10]. A detailed discussion on the primary technical challenges is reported in our previous work [2].

Some of the VHEE facilities in Europe have capabilities, are under operation, or are in development, that can be used for FLASH radiation therapy potential applications. Simulations of beam parameters have been performed to explore the VHEE-FLASH irradiation options for further investigation [12,20].

In Europe and other well-developed countries, there has been an emphatic increase in the availability of VHEE accelerators and VHEE-FLASH facilities, undoubtedly directing accelerator research on modern radiotherapy techniques. The major target and interest are related to FLASH radiation therapy [23,29,32], including a fundamental understanding of the biological mechanisms underpinning FLASH sparing in healthy tissue, in parallel with the standardization of accelerator parameters, providing a stable and reliable ultra-high dose rate capable of FLASH effect conditions. Recently, a quantitative simulation study based on the radiolytic oxygen depletion hypothesis was reported to investigate the oxygen depletion effect on cellular response during FLASH irradiation [37]. In this study, the impact of the radiolytic oxygen depletion (ROD) hypothesis proposes that ultra-high dose rate (UHDR) FLASH radiotherapy causes rapid, temporary oxygen depletion in tissues, reducing oxygen's role in DNA damage and thus sparing normal tissues from harm while tumors remain sensitive to treatment. In recent works, it is indicated that oxygen depletion is unlikely at clinically relevant levels or that oxygen's role is more complex, possibly involving reactive oxygen species (ROS) [69].

It is emphasized that accurate and reliable radiation dosimetry is necessary to enable radiobiological studies of the FLASH mechanism and the effects on healthy and tumor cells across the full VHEE clinical energy range, as well as to establish a comparison between facilities that submit a standardized VHEE-FLASH protocol (in terms of beam parameters and irradiation), enabling a radiobiological study of the FLASH mechanism

and healthy and tumor cell effects across the full VHEE clinical energy range [25,45–48]. This will prove to be an important step on the way to the VHEE-FLASH protocol for clinical implementation.

There are only a few accelerator systems, at present, that can operate at the ultra-high dose rates associated with the FLASH effect. Most FLASH studies to date have been performed with experimental very-low-energy electron devices or modified clinical linacs [70,71]. It is necessary to understand the FLASH irradiation dimensions in terms of the technical beam parameters needed to induce the FLASH beam effect. It is also necessary to understand the effects of manipulating the technical beam parameters on the magnitude of the FLASH effect. This knowledge may be used to elucidate the biological mechanism underlying the FLASH effect in irradiated cells and allow for optimization during FLASH radiation therapy in terms of normal tissue sparing for critical organ systems.

In 2021, the CHUV/Lausanne University Hospital team successfully used two electron beams of about 9 MeV (Mobetron/IntraOp and FLASH knife/PMB-Alcen) to treat superficial skin cancers and to perform intraoperative treatment on other types of cancer [72]. A sequential important approach is the established VHEE facility CLEAR at CERN, aiming to provide a very-high-energy electron FLASH beam that can deliver high doses at high dose rates to relatively large volumes and deep-seated tumors. Additional studies for the treatment planning started some years ago [73,74]. More recent articles review treatment planning for VHEE relative to VMA, clarifying the potential benefit of the modality for a beam energy range of 50–250 MeV [75] or focusing on dosimetric properties and beam delivery for beam energies of 50–400 MeV [7]. In a newly relevant article, the VHEE treatment planning outperformed photon VMAT in sparing organs-at-risk (OARs) while maintaining or improving target coverage, underlining a promising future benefit of the VHEE FLASH radiation therapy [76].

Author Contributions: Conceptualization, N.G. and E.G.; design and methodology, N.G.; software, N.G.; validation, N.G. and E.G.; formal analysis, N.G.; investigation, E.G.; resources, E.G.; data curation, N.G.; writing—original draft preparation, N.G.; writing—review and editing, E.G.; visualization, N.G.; supervision, E.G.; project administration, E.G.; funding acquisition, E.G. All authors have read and agreed to the published version of the manuscript.

Funding: This research was funded by EC grant number 101079773.

Data Availability Statement: The original contributions presented in this study are included in the article. Further inquiries can be directed to the corresponding author.

Acknowledgments: This work was supported in part by funding from the European Union’s Horizon 2020 research and innovation programme EuPRAXIA PP under grant agreement No. 101079773. The contents of this work reflect only the view of the authors. The European Commission is not responsible for any use that may be made of the information it contains. The authors are grateful to Emmanuil Trachanas for his simulation work on the ASTRA code and to Anna Giribono for her support on the TW C-band structures field map.

Conflicts of Interest: The authors declare no conflicts of interest.

References

1. Abdel-Wahab, M.; Gondhowiardjo, S.S.; Rosa, A.A.; Lievens, Y.; El-Haj, N.; Rubio, J.A.P.; Ben Prajogi, G.; Helgadottir, H.; Zubizarreta, E.; Meghzifene, A.; et al. Global Radiotherapy: Current Status and Future Directions—White Paper. *JCO Glob. Oncol.* **2021**, *7*, 827–842. [\[CrossRef\]](#)
2. Gazis, N.; Bignami, A.; Trachanas, E.; Moniaki, M.; Gazis, E.; Bandekas, D.; Vordos, N. Simulation Dosimetry Studies for FLASH Radio Therapy with Ultra-High-Dose Rate (UHDR) Beam. *Quantum Beam Sci.* **2024**, *8*, 13. [\[CrossRef\]](#)
3. Gianfaldoni, S.; Gianfaldoni, R.; Wollina, U.; Lotti, J.; Tchernev, G.; Lotti, T. An Overview on Radiotherapy: From Its History to Its Current Applications in Dermatology. *Open Access Mac. J. Med. Sci.* **2017**, *5*, 521. [\[CrossRef\]](#) [\[PubMed\]](#)

4. Birindelli, G. Entropic Model for Dose Calculation in External Beam Radiotherapy and Brachytherapy. Ph.D. Thesis, Université de Bordeaux, Talence, France, 2011. Available online: <https://tel.archives-ouvertes.fr/tel-03214566> (accessed on 10 September 2025).
5. Tsujii, H. Overview of Carbon-ion Radiotherapy. *J. Phys. Conf. Ser.* **2017**, *777*, 012032. [\[CrossRef\]](#)
6. Tian, X.; Liu, K.; Hou, Y.; Cheng, J.; Zhang, J. The evolution of proton beam therapy: Current and future status (Review). *Mol. Clin. Oncol.* **2017**, *8*, 15–21. [\[CrossRef\]](#) [\[PubMed\]](#)
7. Panaino, C.M.V.; Piccinini, S.; Andreassi, M.G.; Bandini, G.; Borghini, A.; Borgia, M.; Di Naro, A.; Labate, L.U.; Maggiulli, E.; Portaluri, M.G.A.; et al. Very High-Energy Electron Therapy Toward Clinical Implementation. *Cancers* **2025**, *17*, 181. [\[CrossRef\]](#)
8. Gagnebin, S.; Twerenbold, D.; Pedroni, E.; Meer, D.; Zenklusen, S.; Bula, C. Experimental determination of the absorbed dose to water in a scanned proton beam using a water calorimeter and an ionization chamber. *Nucl. Instrum. Methods Phys. Res. Sect. B Beam Interact. Mater. At.* **2010**, *268*, 524–528. [\[CrossRef\]](#)
9. Bourhis, J.; Sozzi, W.J.; Jorge, P.G.; Gaide, O.; Bailat, C.; Duclos, F.; Patin, D.; Ozsahin, M.; Bochud, F.; Germond, J.F.; et al. Clinical translation of FLASH radiotherapy: Why and how? *Radiother. Oncol.* **2019**, *139*, 11–17. [\[CrossRef\]](#)
10. Pratz, G.; Kapp, D.S. A computational model of radiolytic oxygen depletion during FLASH irradiation and its effect on the oxygen enhancement ratio. *Phys. Med. Biol.* **2019**, *64*, 185005. [\[CrossRef\]](#) [\[PubMed\]](#)
11. Favaudon, V.; Caplier, L.; Monceau, V.; Pouzoulet, F.; Sayarath, M.; Fouillade, C.; Poupon, M.F.; Brito, I.; Hupe, P.; Bourhis, J.; et al. Ultrahigh dose-rate FLASH irradiation increases the differential response between normal and tumor tissue in mice. *Sci. Transl. Med.* **2014**, *6*, 245–293. [\[CrossRef\]](#) [\[PubMed\]](#)
12. Naceur, A.; Bienvenue, C.; Romano, P.; Chilian, C.; Carrier, J.-F. Extending deterministic transport capabilities for very-high and ultra-high energy electron beams. *Sci. Rep.* **2024**, *14*, 2796. [\[CrossRef\]](#)
13. Gamba, D.; Corsini, R.; Curt, S.; Doeber, S.; Frabolini, W.; Mcmonagle, G.; Skowronski, P.K.; Tecket, F.; Zeeshan, S.; Adli, E.; et al. The CLEAR user facility at CERN. *Nucl. Instrum. Methods Phys. Res. Sect. A Accel. Spectrometers Detect. Assoc. Equip.* **2018**, *909*, 480–483. [\[CrossRef\]](#)
14. Marchand, D. A new platform for research and applications with electrons: The PRAE project. *EPJ Web Conf.* **2017**, *138*, 01012. [\[CrossRef\]](#)
15. Delorme, R.; Marchand, D.; Vallerand, C. The PRAE Multidisciplinary Project. *Nucl. Phys News* **2019**, *29*, 32–35. [\[CrossRef\]](#)
16. Han, Y.; Faus-Golfe, A.; Vallerand, C.; Bai, B.; Duchesne, P.; Prezado, Y.; Delorme, R.; Poortmans, P.; Favaudon, V.; Fouillade, C.; et al. Optics design and beam dynamics simulation for a VHEE radiobiology beam line at PRAE accelerator. In Proceedings of the 10th International Particle Accelerator Conference; IPAC2019, Melbourne, Australia, 19–24 May 2019. [\[CrossRef\]](#)
17. Angal-Kalinin, D.; Boogert, S.; Jones, J.K. Potential of the CLARA test facility for VHEE rationally research. *Front. Phys.* **2024**, *12*, 1496850. [\[CrossRef\]](#)
18. Ferrario, M.; Alesini, D.; Anania, M.; Bacci, A.; Bellaveglia, M.; Bogdanov, O.; Boni, R.; Castellano, M.; Chiadroni, E.; Cianchi, A.; et al. SPARC_LAB present and future. *Nucl. Instrum. Methods Phys. Res. Sect. B Beam Interact. Mater. At.* **2013**, *309*, 183–188. [\[CrossRef\]](#)
19. Small, K.L.; Angal-Kalinin, D.; Jones, J.K.; Jones, R.J. VHEE facilities I Europe with the potential for FLASH dose irradiation; Conspectus and dose rate parameterization. *Nucl. Instrum. Methods Phys. Res. Sect. B Beam Interact. Mater. At.* **2025**, *565*, 165752. [\[CrossRef\]](#)
20. Masilela, T.A.M.; Delorme, R.; Prezado, Y. Dosimetry and radioprotection evaluations of very-high energy electron beams. *Sci. Rep.* **2021**, *11*, 20184. [\[CrossRef\]](#) [\[PubMed\]](#)
21. Nakajima, K.; Yuan, J.; Chen, L.; Sheng, Z. Laser-driven very high energy electron/photon beam radiation therapy in conjunction with a robotic system. *Appl. Sci.* **2015**, *5*, 1–20. [\[CrossRef\]](#)
22. DesRosiers, C.; Moskvina, V.; Cao, M.; Joshi, C.J.; Langer, M. Laser-plasma generated very high energy electrons in radiation therapy of the prostate. *Proc. SPIE* **2008**, *6881*, 49–62. [\[CrossRef\]](#)
23. Kokurewicz, K.; Welsh, C.H.; Brunetti, E.; Wiggins, S.M.; Boyd, M.; Sorensen, A.; Chalmers, A.; Schettino, G.; Subiel, A.; DesRosiers, C.; et al. Laser-plasma generated very high energy electrons (VHEEs) in radiotherapy. *Proc. SPIE* **2017**, *10239*, 61–69. [\[CrossRef\]](#)
24. Poppinga, D.; Kranzer, R.; Farabolini, W.; Gilardi, A.; Corsini, R.; Wyrwoll, V.; Looe, H.K.; Delfs, B.; Gabrisch, L.; Poppe, L. VHEE beam dosimetry at CERN linear electron accelerator for research under ultra-high dose rate conditions. *Biomed. Phys. Eng. Express* **2020**, *7*, 015012. [\[CrossRef\]](#) [\[PubMed\]](#)
25. Kokurewicz, K.; Brunetti, E.; Welsh, G.H.; Wiggins, S.M.; Boyd, M.; Sorensen, A.; Chalmers, A.J.; Schettino, G.; Subiel, A.; DesRosiers, C.; et al. Focused very high-energy electron beams as a novel radiotherapy modality for producing high-dose volumetric elements. *Sci. Rep.* **2019**, *9*, 10837. [\[CrossRef\]](#) [\[PubMed\]](#)
26. Kaiser, A.; Eley, J.G.; Onyeuku, N.E.; Rice, S.R.; Wright, C.C.; McGovern, N.E.; Sank, M.; Zhu, M.; Vujaskovic, Z.; Simone, C.B.; et al. Proton Therapy Delivery and Its Clinical Application in Select Solid Tumor Malignancies. *J. Vis. Exp.* **2019**, *144*, e58372. [\[CrossRef\]](#)
27. Giuliano, L.; Franciosini, G.; Palumbo, L.; Aggar, L.; Dutreix, M.; Faillace, L.; Favaudon, V.; Felici, G.; Galante, F.; Mostacci, A.; et al. Characterization of Ultra-High-Dose Rate Electron Beams with Electron Flash Linac. *Appl. Sci.* **2023**, *13*, 631. [\[CrossRef\]](#)

28. Montay-Gruel, P.; Petersson, K.; Jaccard, M.; Boivin, G.; Germond, J.-F.; Petit, B.; Doenlen, R.; Favaudon, V.; Bochud, F.; Bailat, C.; et al. Irradiation in a flash: Unique sparing of memory in mice after whole brain irradiation with dose rates above 100 Gy/s. *Radiother. Oncol.* **2017**, *124*, 365–369. [[CrossRef](#)] [[PubMed](#)]
29. Desrosiers, C.; Moskvina, V.; Bielajew, A.F.; Papiez, L. 150–250 MeV electron beams in radiation therapy. *Phys. Med. Biol.* **2000**, *45*, 1781–1805. [[CrossRef](#)]
30. Chaudhary, P.; Shukla, S.K.; Suman, S. Editorial: Multifaceted Approaches Combining Low or High LET Radiation and Pharmacological Interventions in Cancer and Radioprotection: From Bench to Bedside. *Front. Oncol.* **2022**, *12*, 880607. [[CrossRef](#)] [[PubMed](#)]
31. Kristensen, L.; Rohrer, S.; Hoffmann, L.; Præstegaard, L.H.; Ankjærgaard, C.; Andersen, C.E.; Kanouta, E.; Johansen, J.G.; Sahlertz, M.; Nijkamp, J.; et al. Electron vs proton FLASH radiation on murine skin toxicity. *Radiother. Oncol.* **2025**, *206*, 110796. [[CrossRef](#)] [[PubMed](#)]
32. Rongo, M.G.; Cavallone, M.; Patriarca, A.; Leite, A.M.; Loap, P.; Favaudon, V.; Crehange, G.; De Marzi, L. Back to the Future: Very High-Energy Electrons (VHEEs) and their potential applications in Radiation Therapy. *Cancers* **2021**, *13*, 4942. [[CrossRef](#)]
33. Hogstrom, K.R.; Almond, P.R. Review of electron beam therapy physics. *Phys. Med. Biol.* **2006**, *51*, R455–R489. [[CrossRef](#)] [[PubMed](#)]
34. Mueller, S.; Fix, M.K.; Henzen, D.; Frei, D.; Frauchiger, D.; Loessl, K.; Stampanoni, M.F.M.; Manser, P. Electron beam collimation with a photon MLC for standard electron treatments. *Phys. Med. Biol.* **2017**, *63*, 025017. [[CrossRef](#)] [[PubMed](#)]
35. Krempien, R.; Roeder, F. Intraoperative radiation therapy (IORT) in pancreatic cancer. *Radiat. Oncol.* **2017**, *12*, 8. [[CrossRef](#)]
36. Vozenin, M.-C.; De Fornel, P.; Petersson, K.; Favaudon, V.; Jaccard, M.; Germond, J.-F.; Petit, B.; Burki, M.; Ferrand, G.; Patin, D.; et al. The Advantage of FLASH Radiotherapy Confirmed in Mini-pig and Cat-cancer Patients. *Clin. Cancer Res.* **2018**, *25*, 35–42. [[CrossRef](#)] [[PubMed](#)]
37. Vozenin, M.-C.; Hendry, J.; Limoli, C. Biological Benefits of Ultra-high Dose Rate FLASH Radiotherapy: Sleeping Beauty Awoken. *Clin. Oncol.* **2019**, *31*, 407–415. [[CrossRef](#)]
38. Wilson, J.D.; Hammond, E.M.; Higgins, G.S.; Petersson, K. Ultra-High Dose Rate (FLASH) Radiotherapy: Silver Bullet or Fool's Gold? *Front. Oncol.* **2020**, *17*, 1563. [[CrossRef](#)]
39. Gazis, N.; Bignami, A.; Trachanas, E.; Alexopoulos, T.; Telali, I.; Apostolopoulos, T.; Pramataris, K.; Karagiannaki, K.; Kotsopoulos, D.; Gazis, E. The Innovative FEL design by the CompactLight collaboration. *J. Phys. Conf. Ser.* **2022**, *2375*, 012006. [[CrossRef](#)]
40. Gazis, N.; Tanke, E.; Apostolopoulos, T.; Pramataris, K.; Rochow, R.; and Gazis, E. Light source in Europe-Case Study: The CompactLight collaboration. *Instruments* **2019**, *3*, 43. [[CrossRef](#)]
41. EuPRAXIA PP Project. Available online: <https://www.eupraxia-pp.org/> (accessed on 10 September 2025).
42. Giribono, A.; Alesini, D.; Bacci, A.; Bellaveglia, M.; Cardelli, F.; Chiadroni, E.; Del Dotto, A.; Faillace, L.; Ferrario, M.; Gallo, A.; et al. Electron beam analysis and sensitivity studies for the EuPRAXIA@SPARC LAB RF injector. *J. Phys. Conf. Ser.* **2024**, *2687*, 032022. [[CrossRef](#)]
43. Bayart, E.; Flacco, A.; Delmas, O.; Pommarel, L.; Levy, D.; Cavallone, M.; Megnin-Chanet, F.; Deutsch, E.; and Malka, V. Fast dose fractionation using ultra-short laser accelerated proton pulses can increase cancer cell mortality, which relies on functional PARP1 protein. *Sci. Rep.* **2019**, *9*, 10132. [[CrossRef](#)]
44. Zhu, H.; Li, J.; Deng, X.; Qiu, R.; Wu, Z.; Zhang, H. Modeling of cellular responses after FLASH irradiation: A quantitative analysis based on the radiolytic oxygen depletion hypothesis. *arXiv* **2021**, arXiv:2105.13138. [[CrossRef](#)]
45. Rieker, V.F.; Farabolini, W.; Corsini, R.; Batchman, J.J.; Korysko, P.; Dyks, L.A. VHEE high dose rate dosimetry studies in CLEAR. In Proceedings of the 13th International Particle Accelerator Conference, Bangkok, Thailand, 12–17 June 2022. [[CrossRef](#)]
46. Lagzda Aangal-Kalinin, D.; Jones, J.; Aitkenhead, A.; Kirkby, K.J.; MacKay, R.; Van Herk, M.; Farabolini, W.; Zeeshan, S.; Jones, R.M. Influence of heterogeneous media on Very High Energy Electron (VHEE) penetration and a Monte Carlo-based comparison with existing radiotherapy modalities. *Nucl. Instrum. Methods Phys. Res. Sect. B Beam Interact. Mater. At.* **2020**, *482*, 70–81. [[CrossRef](#)]
47. Grunwald, K.; Desch, K.; Elsner, D.; Proft, D.; Thome, L. Dose simulation of Ultra-High Energy Electron beams for novel FLASH radiation therapy applications. In Proceedings of the 14th International Particle Accelerator Conference, Venice, Italy, 7–12 May 2023; pp. 4993–4995. [[CrossRef](#)]
48. Papiez, L.; Desrosiers, C.M.; Moskvina, V. Very high energy electrons (50–250 MeV) and Radiation Therapy. *Technol. Cancer Res. Treat.* **2002**, *1*, 1050110. [[CrossRef](#)]
49. Borghini, A.; Labate, L.; Piccinini, S.; Panaino, C.M.V.; Andreassi, M.G.; Gizzi, L.A. FLASH radiotherapy: Expectations, Challenges and current knowledge. *Int. J. Mol. Sci.* **2024**, *25*, 2546. [[CrossRef](#)]
50. Maxim, P.G.; Tantawi, S.G.; Loo, B.W. PHASER: A platform for clinical translation of FLASH cancer radiotherapy. *Radiother. Oncol.* **2019**, *139*, 28–33. [[CrossRef](#)] [[PubMed](#)]
51. Korysko, P.; Dosanjh, M.; Dyks, L.A.; Bateman, J.J.; Robertson, C.; Corsini, R.; Farabolini, W.; Gilardi, A.; Sjobak, K.N.; Rieker, V. Updates, status and experiments of CLEAR, the CERN Linear Electron Accelerator for Research. In Proceedings of the 13th International Particle Accelerator Conference, Bangkok, Thailand, 12–17 June 2022. [[CrossRef](#)]

52. Burkart, F.; Assmann, R.W.; Dinter, H.; Jaster-Merz, S.; Kuropka, W.; Mayer, F.; Stacey, B.; Vinatier, T. The ARES linac at DESY. In Proceedings of the 31st International Linear Accelerator Conference, Liverpool, UK, 28 August–2 September 2022. [CrossRef]
53. Vinatier, T.; Assmann, R.W.; Burkart, F.; Dinter, H.; Jaster-Merz, S.; Kellermeier, M.; Kuropka, W.; Mayer, F.; Stacey, B. Characterization of relativistic electron bunch duration and travelling wave structure phase velocity based on momentum spectra. *Phys. Rev. Accel. Beams* **2023**, *27*, 022801. [CrossRef]
54. Clarke, J.A.; Angal-Kalinin, D.; Bliss, N.; Buckley, R.; Buckley, S.; Cash, R.; Corlett, P.; Cowie, L.; Cox, G.; Diakun, G.P.; et al. CLARA Conceptual Design Report. *Sci. Technol. Facil. Counc.* **2013**, *9*, T05001. Available online: https://www.astec.stfc.ac.uk/Pages/CLARA_CDRv2.pdf (accessed on 10 September 2025). [CrossRef]
55. Angal-Kalinin, D.; Bainbridge, A.; Brynes, A.D.; Buckley, R.; Buckley, S.; Burt, G.C.; Cash, R.; Castaneda, H.M.; Christie, D. Design, specifications, and first beam measurements of the compact linear accelerator for research and applications front end. *Phys. Rev. Accel. Beams* **2020**, *23*, 044801. [CrossRef]
56. Angal-Kalinin, D.; Bainbridge, A.; Jones, J.K.; Pacey, T.H.; Saveliev, Y.M.; Snedden, E.W. The design of the Full Energy Beam Exploitation (FEBE) beamline on CLARA. In Proceedings of the 31st International Linear Accelerator Conference, Liverpool, UK, 28 August–2 September 2022. [CrossRef]
57. Snedden, E.W.; Angal-Kalinin, D.; Bainbridge, A.R.; Brynes, A.D.; Buckley, S.R.; Dunning, D.J.; Henderson, J.R.; Jones, J.K.; Middleman, K.J.; Overton, T.J.; et al. Specification and design for full energy beam exploitation of the compact linear accelerator for research applications. *Phys. Rev. Accel. Beams* **2024**, *27*, 041602. [CrossRef]
58. Palumbo, L.; Bosco, F.; Carillo, M.; Chiadroni, E.; De Arcangelis, D.; De Gregorio, A.; Ficcadeni, I.; Francescone, D.; Franciosini, G.; Guliano, L.; et al. SAFEST: A compact C-band linear accelerator for VHEE-FLASH radiotherapy. In Proceedings of the 14th International Particle Accelerator Conference, Venice, Italy, 7–12 May 2023. [CrossRef]
59. Guiliano, L.; Carillo, M.; Chiadroni, E.; De Arcangelis, D.; De Gregorio, A.; Ficcadeni, I.; Francescone, D.; Franciosini, G.; Magi, M.; Migliorati, M.; et al. SAFEST project, a compact C-band RF linac for VHEE FLASH radiotherapy. In Proceedings of the 15th International Particle Accelerator Conference, Nashville, TN, USA, 19–24 May 2024. [CrossRef]
60. Flöttmann, K. *ASTRA, A Space Charge Tracking Algorithm*, Version 3.2; DESY: Hamburg, Germany, 2017. Available online: https://www.desy.de/~mpyflo/Astra_manual/Astra-Manual_V3.2.pdf (accessed on 10 September 2025).
61. Bhat, C.M.; Carneiro, J.-P.; Fliller, R.P.; Kazakevich, G.; Ruan, J.; Santucci, J. Envelope and multi-slit emittance measurements at Fermilab A0-photoinjector and comparison with simulations. In Proceedings of the PAC07, Albuquerque, NM, USA, 25–29 June 2007; p. THPMN097. Available online: <https://accelconf.web.cern.ch/p07/papers/THPMN097.pdf> (accessed on 10 September 2025).
62. Prat, E.; Aiba, M.; Bettoni, S.; Beutner, B.; Reiche, S.; Schietinger, T. Emittance measurements and minimization at the SwissFEL injector test facility. *Phys. Rev. ST Accel. Beams* **2014**, *17*, 104401. [CrossRef]
63. Latini, G.; Chiadroni, E.; Mostacci, A.; Martinelli, V.; Serenellini, V.; Silvi, G.J.; Pioli, S. Design of machine learning-based algorithms for virtualized diagnostic on SPARC_LAB accelerator. *Photonics* **2024**, *11*, 516. [CrossRef]
64. FLUKA. Available online: <https://www.fluka.eu> (accessed on 10 September 2025).
65. Rata, R.; Lee, S.C.; Barlow, R.J. FLUKA simulations for radiation protection at 3 different facilities. In Proceedings of the IPAC2016, 7th International Particle Accelerator Conference, Busan, Republic of Korea, 10 May 2016; p. TUPOY018. [CrossRef]
66. Böhlen, T.T.; Germond, J.-F.; Desorgher, L.; Veres, I.; Bratel, A.; Landström, E.; Engwall, E.; Herrera, F.G.; Ozsahin, E.M.; Bourhis, J.; et al. Very high-energy electron therapy as light-particle alternative to transmission proton FLASH therapy—An evaluation of dosimetric performances. *Radiother. Oncol.* **2024**, *194*, 110177. [CrossRef] [PubMed]
67. Khallouqi, A.; Halimi, A.; El Rhazouani, O.; Mesradi, M.R.; El Mansouri, K.; Sekkat, H. Comparing tissue-equivalent properties of polyester and epoxy resins with PMMA material using Gate/Geant4 simulation toolkit. *Radiat. Phys. Chem.* **2024**, *220*, 111702. [CrossRef]
68. Queralt, X. Radiation Safety, Chapter II.12, CERN Yellow Reports: Monographs, CERN-2024-003. In *The Joint Universities Accelerator School (JUAS)—Courses and Exercises, Proceedings of the 30th Joint Universities Accelerator School (JUAS), Geneva, Switzerland, 28 November 2024*; Métral, E., Ed.; CERN: Geneva, Switzerland, 2024. [CrossRef]
69. Scarmelotto, A.; Delprat, V.; Michiels, C.; Lucas, S.; Heuskin, A.-C. The oxygen puzzle in FLASH radiotherapy: A comprehensive review and experimental outlook. *Clin. Transl. Radiat. Oncol.* **2024**, *49*, 100860. [CrossRef]
70. Gazis, N.; Tanke, E.; Trachanas, E.; Apostolopoulos, T.; Karagiannaki, A.; Pramataris, K.; Telali, I.; Tzanetou, K.; Gazis, E. Photocathode study of the CompactLight Collaboration for a novel XFEL development. *Int. J. Mod. Phys. Conf. Ser.* **2020**, *50*, 2060007. [CrossRef]
71. Schuler, E.; Acharya, M.; Montay-Gruel, P.; Loo, B., Jr.; Vozenin, M.-C.; Maxim, G.P. Ultra-high dose rate electron beams and the FLASH effect: From preclinical evidence to a new radiotherapy paradigm. *Med. Phys.* **2022**, *49*, 2082–2095. [CrossRef]
72. Wu, Y.F.; No, H.J.; Breikreutz, D.Y.; Mascia, A.E.; Moeckli, R.; Bourhis, J.; Schüler, E.; Maxim, P.G.; Loo, B.W. Technological basis for clinical trials in FLASH radiation therapy: A review. *Appl. Rad. Oncol.* **2021**, *10*, 6–14. Available online: https://cdn.agilitycms.com/applied-radiation-oncology/PDFs/issues/ARO_06-21_all.pdf (accessed on 10 September 2025). [CrossRef]

73. Schüler, E.; Eriksson, K.; Hynning, E.; Hancock, S.L.; Hiniker, S.M.; Bazalova-Carter, M.; Wong, T.; Le, Q.; Loo, B.W.; Maxim, P.G. Very high-energy electron (VHEE) beams in radiation therapy; treatment plan comparison between VHEE, VMAT, and PPBS. *Med. Phys.* **2017**, *44*, 2544–2555. [[CrossRef](#)] [[PubMed](#)]
74. Bazalova-Carter, M.; Qu, B.; Palma, B.; Hårdemark, B.; Hynning, E.; Jensen, C.; Maxim, P.G.; Loo, B.W. Treatment planning for radiotherapy with very high-energy electron beams and comparison of VHEE and VMAT plans. *Med. Phys.* **2015**, *42*, 2615–2625. [[CrossRef](#)] [[PubMed](#)]
75. Bedford, J.L.; Oelfke, U. Treatment planning for very high energy electrons: Studies that indicate the potential of the modality. *Phys. Imaging Radiat. Oncol.* **2024**, *32*, 100670. [[CrossRef](#)] [[PubMed](#)]
76. D’Andrea, F.S.; Chuter, R.; Aitkenhead, A.H.; MacKay, R.I.; Jones, R.M. Comparative treatment planning of very high-energy electrons and photon volumetric arc therapy: Optimising energy and beam parameters. *Phys. Imaging Radiat. Oncol.* **2025**, *33*, 100732. [[CrossRef](#)] [[PubMed](#)]

Disclaimer/Publisher’s Note: The statements, opinions and data contained in all publications are solely those of the individual author(s) and contributor(s) and not of MDPI and/or the editor(s). MDPI and/or the editor(s) disclaim responsibility for any injury to people or property resulting from any ideas, methods, instructions or products referred to in the content.